Int. J. Heat Mass Transfer. Vol. 25, No. 5, pp. 683–690, 1982
Printed in Great Britain

0017 9310/82/050683–08 $03.00/0
Pergamon Press Ltd.

A STUDY OF BOILING OUTSIDE A TUBE BUNDLE USING HIGH SPEED PHOTOGRAPHY

K. CORNWELL and R. B. SCHÜLLER
Department of Mechanical Engineering, Heriot–Watt University, Edinburgh, U.K.

(*Received* 5 *May* 1981 *and in final form* 16 *November* 1981)

Abstract—A high speed film of boiling outside tubes near the top of a horizontal reboiler tube bundle reveals a multitude of small bubbles which grow rapidly while sliding up the side of the tube. These bubbles originate from both the main stream and from nucleation sites at the base of the tube. The measured growth rate correlates well with theory based on an evaporating microlayer under the bubble. It is shown that sliding bubbles can account for the enhancement of heat transfer observed at the upper tubes of bundles.

NOMENCLATURE

a, mean diameter of contact area;
b, length of liquid layer;
C_d, drag coefficient of sphere;
D, mean bubble diameter;
F_b, buoyancy force;
F_d, drag force;
F_s, surface tension force;
g, acceleration due to gravity;
h, heat transfer coefficient;
h_{fg}, enthalpy of vaporisation;
k_f, thermal conductivity of liquid;
M, function of θ_m;
$\dot{m}$, mass flow rate;
N, function of θ_m;
n_{sb}, mean number of bubbles per unit area at any one time;
$\dot{n}_{sb}$, mean number of sliding bubbles per unit time and area;
P, mean proportion of the tube circumference occupied by sliding bubbles;
Q, heat flow rate;
q, heat flow rate per unit total area;
q_{sb}, heat flux due to sliding bubbles;
Re, Reynolds number for sphere, $\rho_f U_b D/\mu_f$;
r, radius (defined in Fig. 7);
t, time;
T_{sat}, saturation temperature;
T_w, wall temperature;
U_b, velocity of sliding bubble;
U_s, velocity of liquid in main stream;
x, distance normal to flow direction;
z, distance in flow direction;

Greek symbols

ΔT_{sat}, wall superheat, $T_w - T_{sat}$;
ΔU, velocity difference, $U_s - U_b$;
δ, liquid layer thickness;
θ, local liquid contact angle;
θ_a, advancing liquid contact angle;
θ_m, mean liquid contact angle [defined in Fig. 7 and equation (10)];
μ_f, liquid viscosity;
ρ_f, liquid density;
σ, surface tension;
τ_{sb}, time period bubble slides on surface;
ϕ, angle defined in Fig. 8.

1. INTRODUCTION

THE WORK described in this paper arose from the need to determine the mechanism which causes an anomalous increase in the boiling heat transfer coefficient in the upper tubes of a bundle. The experimental work is based on the same reboiler slice described in Leong and Cornwall [1]. The bundle contains 241 electrically heated, 25.4 mm long tubes of 19 mm dia and 25.4 mm square pitch, and the test fluid is R113 at 1 atm. and 48°C. Lines of constant heat transfer coefficient within the section, drawn by interpolation between the measured values at each tube, are given for a uniform heat flux of 20 kWm^{-2} in Fig. 1 and for other heat fluxes in ref. [1]. It is shown in Cornwell *et al.* [2] that the high h values at the top of the bundle cannot be entirely accredited to the influence of fluid velocity on the flow boiling and that some additional heat transfer mechanism is responsible.

Figure 2 shows the type of flow occurring near the top of the bundle at a heat flux of 20 kWm^{-2} (this flux yields a vapour production rate per unit area for R113 which is typical of the conditions in industrial bundles). Ciné films show a large number of bubbles that grow while sliding around the side of the tube. These bubbles either impinge on the side from the main stream or slide up from nucleation sites near the base of the tube.

Figure 3 shows the comparatively low bubble density occurring around a similar tube under pool boiling conditions at a heat flux greater by a factor of 2.5. Here also ciné films reveal the importance of sliding bubbles, and their influence on heat transfer is at present under study. This paper is restricted to the

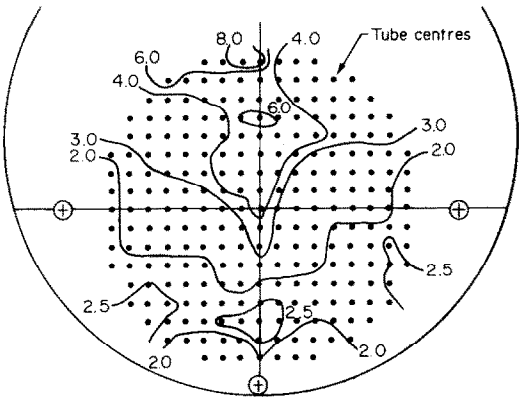

FIG. 1. Iso-h lines (kW m^2 K^{-1}) at a heat flux of 20 kW m^{-2} in the reboiler tube bundle.

observation and initial analysis of sliding bubbles in the upper tubes of the tube bundle.

Since the observation of sliding bubbles by Gunther [3] in 1951, a number of studies have been made of growing, sliding and collapsing bubbles under subcooled flow boiling conditions e.g. ref. [10]. The existence of a liquid microlayer which dries out under the bubble, similar to that sometimes observed in pool boiling, was shown by Anderson and Minns [4]. Very recently Mori [12] has reported thin layers under sliding bubbles growing in uniform superheat at zero gravity. There was no indication of the layers drying out under the experimental conditions used.

For the case of tube bundles, both Nakajima [5] and Niels [6] observed large bubbles about the size of the tube clearance and analysed the heat transfer in a similar way to the evaporation of a liquid layer under bubbles in slug flow. These large bubbles were not observed in our experiments using R113 in much larger tube bundles and the photographic study indicated a strong resemblance to the sliding bubbles reported by Anderson and Minns [4].

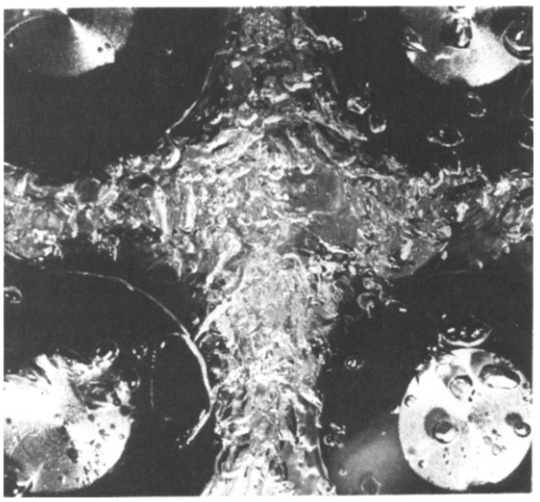

FIG. 2. Boiling between the upper tubes of a bundle at 20 kW m^{-2} (R113, 1 atm., 19 mm dia).

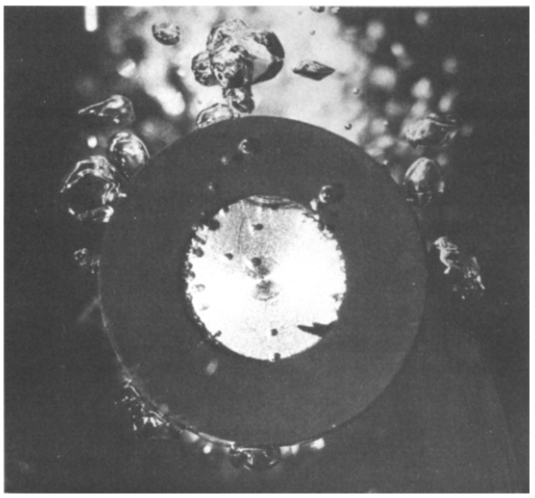

FIG. 3. Pool boiling on a tube at 50 kW m^{-2} (R113, 1 atm., 19 mm dia).

2. THE SLIDING BUBBLE MICROLAYER

The object of the following analysis is to find the magnitude of the liquid layer thickness under a growing bubble sliding up a vertical surface at constant velocity U_b. The observed high contact angle at the advancing (lower) edge of the bubble suggests a *dry spot* on the surface. Similar bubble shapes and contact angles were observed by Williams and Mesler [11] for bubbles sliding up a vertical surface due to buoyancy. The contact area of the bubble is roughly ellipsoidal as shown in Fig. 4 and the area of the microlayer is taken as the product of the mean contact diameter of approx. a and a layer length b, to be determined.

Consider the control volume a, dz, δ moving along the surface a distance z from the moving reference frame z_0. The difference in mass flow rate into and out of the control volume is equal to the mass evaporated. Thus

$$\left(\frac{\partial \dot{m}}{\partial z}\right) \mathrm{d}z = \frac{\mathrm{d}Q}{h_{fg}}$$

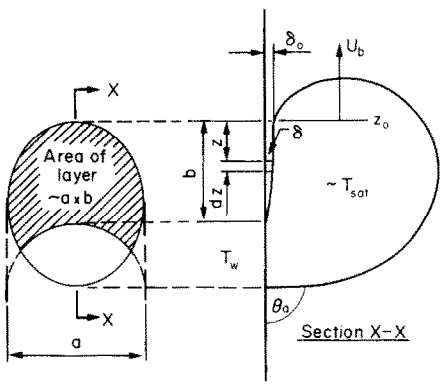

FIG. 4. Arrangement of sliding bubble with microlayer.

where dQ is the incremental heat flow rate. The heat flow through the control volume is a function of time. Calculation shows that for the mean thickness (2 μm) of R113 involved here, the steady-state distribution is approached within 0.1 ms and it is therefore considered a reasonable approximation to assume linear conduction across the layer. (In contrast the microlayer existing under some conditions of pool boiling is thicker and, at a mean thickness of, say, 10 μm, the transients do not fade for several milliseconds. It may then be more reasonable to approximate to the case of transient heat flow into an infinite extent of liquid). For linear conduction, assuming the effects of bubble pressure on T_{sat} and local surface cooling on T_w are ignored

$$dQ = -k_f a\, dz \frac{\Delta T_{sat}}{\delta}. \tag{1}$$

Assuming that the very thin layer under the bubble is stationary with respect to the surface the nominal mass flow into the moving control volume is

$$\dot{m} = \rho_f U_b a \delta. \tag{2}$$

Rearrangement and substitution of appropriate boundary condition gives

$$\int_{\delta_0}^{\delta} \delta d\delta = \int_0^z \frac{-k_f \Delta T_{sat}}{\rho_f U_b h_{fg}} dz.$$

That is

$$\delta^2 = \delta_0^2 - \left(\frac{2k_f \Delta T_{sat}}{\rho_f U_b h_{fg}}\right) z$$

and at $z = b$, $\delta = 0$,

$$\delta^2 = \frac{2k_f \Delta T_{sat}}{\rho_f U_b h_{fg}} (b - z). \tag{3}$$

Substitution for δ in equation (1) and integration to give the total heat flow rate to the bubble from the microlayer yields

$$\int_0^Q dQ = a(\tfrac{1}{2} k_f \Delta T_{sat} \rho_f h_{fg} U_b)^{1/2} \int_0^b \left(\frac{1}{b - z}\right)^{1/2} dz,$$

$$Q = 2a(\tfrac{1}{2} k_f \Delta T_{sat} \rho_f h_{fg} U_b b)^{1/2}. \tag{4}$$

For the purposes of this analysis it is assumed that the bubble of mean diameter D grows owing to evaporation of the microlayer only. The assumption means that the transient cooling of the surface during growth, the consideration of vapour at the outer parts of the bubble and the sensible heat content of the layer are all ignored. Examination of pool-boiling microlayer studies (such as Cooper and Lloyd [7]) show that this is not unreasonable under saturated liquid conditions. (This assumption must of course not be confused with the microlayer evaporation proportion of the total heat flux in pool boiling, as the total value includes a large part due to transient conduction during the waiting period.) The expression for the heat flow to the bubble then becomes

$$Q dt = \rho_g h_{fg} (\pi/6)\, d(D)^3. \tag{5}$$

Elimination of Q between equations (4) and (5) and rearrangement gives

$$b = (\pi/12)^2 \frac{2h_{fg} \rho_g^2}{k_f \Delta T_{sat} \rho_f U_b} \left[\frac{1}{a} \frac{d(D^3)}{dt}\right]^2 \tag{6}$$

where the term in the square brackets may be estimated from bubble photographs. The inital microlayer thickness is given by

$$\delta_0 = \left(\frac{2k_f \Delta T_{sat} b}{\rho_f U_b h_{fg}}\right)^{1/2}. \tag{7}$$

The heat flow rate due to the sliding bubble is simply the product of the mass flow rate to the layer and the latent heat

$$Q = (\dot{m})_{z=0} h_{fg} = \rho_f U_b a \delta_0 h_{fg}.$$

If n_{sb} is the average number of sliding bubbles per unit area *at any one time*, the heat flux q_{sb} (based on total area) due to sliding bubbles is

$$q_{sb} \simeq n_{sb} \rho_f h_{fg} U_b a \delta_0. \tag{8}$$

3. PHOTOGRAPHIC STUDY

The photographic study involved still shots of the flow boiling using short duration electronic flash and a high speed ciné study using a Hadland "Hyspeed" rotating prism camera. The film analysed here shows bubbly-flow boiling of R113 similar to that shown in Fig. 2 at $q = 20\,kWm^{-2}$ and nominal $h = 6\,kWm^{-2}K^{-1}$ between the third and fourth rows from the top of the bundle described earlier. Although many thousand frames were available for analysis, only parts of the film showed a clear view into the boiling region owing to visual disturbance by bubbles in the foreground and large light intensity changes caused by the flow. In this section the path of various bubbles over a clear period of 10 ms is examined. The mean film speed over this period is 3600 frames s^{-1} and the mean liquid velocity in the vertical gap between the tubes is $1.2 \pm 30\%$ m s^{-1}. (This value is the average of 10 measurements of the movement of small pieces of paper or bubbles, and the accuracy is adversely affected by the general turbulence and the rapid acceleration and deceleration as the fluid flows through the gap between the tubes.)

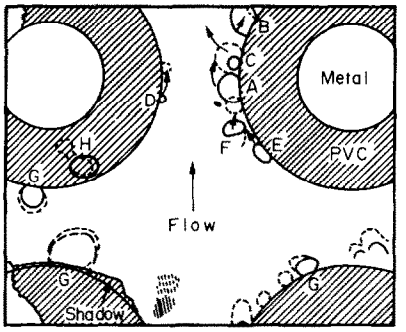

FIG. 5. Sketch showing changes occurring over a period of 3.3 ms (Frames 13–25, Table 1).

Figure 5 is a tracing from the ciné film showing the movement of various bubbles. (The scale may be judged from the 19.05 mm dia and pitch of 24.1 mm.) Bubbles A and B are typical of those that slide along the surface and grow simultaneously and these two are analysed in detail later. C slides along the surface with very little growth and is swept into the main stream. D is similar to C, but smaller (0.5 mm dia) and is not transferred to the main flow in the period studied. E is initially fairly clear and appears almost hemispherical suggesting growth under inertial restraint. In the latter part of the period it seems to collapse or be destroyed by the surrounding turbulent flow. F follows the opposite process to C, D and E, originating in the main stream, impinging on the surface and forming a distinct sliding bubble before moving out of focus. The various bubbles labelled G are stationary and merely grow or change shape over the period involved. Vapour (H) trapped between the end gasket and the glass is very noticeable in the film but has an insignificant effect on the overall flow.

Returning to bubbles A and B, these can be analysed in more detail as their growth rate can be roughly estimated from enlargements of the film. Values of the mean diameter D and the bubble height x from the surface are given in Table 1. The contact area diameter a is estimated from D and x by assuming the bubble surface is spherical (Fig. 7). The contact area diameter can only be estimated from x and the assumption for this purpose that the bubble has a spherical surface of diameter D. This is a major factor in limiting the accuracy of the analysis. The mean velocities of the bubbles are found from the position–time plot in Fig. 6. (The overall accuracy does not warrant consideration of the velocity distribution or the tube curvature). Substitution of the bubble growth parameter obtained from Fig. 6 and a ΔT_{sat} value of 3.33°C (from q/h) into equations (6) and (7) allows calculation of the mean b and δ_0 values given in Fig. 6.

The length b of the microlayer is similar to the contact area diameter over the latter stages of growth and, in view of the assumptions in the analysis, this may be viewed as collaborative evidence that a microlayer under a sliding bubble can account for the observed rapid growth rate. The initial thickness δ_0 of the layer (a few micrometres) is less than the microlayer thickness under some conditions of pool boiling, but similar to that reported under the sliding bubbles analysed by Anderson and Minns [4]. Over part of the contact area, the microlayer thickness is of a similar magnitude to the surface roughness. Over this part, evaporation effectively occurs from remnants of the receding layer remaining in surface indentations and is therefore affected by the complications of the microsurface and the liquid contact angle (see Cornwell, [8]).

4. VELOCITY OF THE SLIDING BUBBLE

The velocity of the bubble may be estimated from a pseudostatic force balance for the case when both the bubble and the liquid velocities are constant and the bubble growth rate is small compared to the translational velocity. Forces acting on the bubble, other than buoyancy, drag and surface tension are ignored. The buoyancy and drag forces may be easily calculated if the bubble is approximated to a segmented sphere as shown in the plan view in Fig. 7. The surface tension force arises owing to the difference between the advancing and retarding contact angles as the bubble slides up the surface. This force is obviously a complicated function of surface effects but may be estimated as follows.

Figure 8 shows the contact area (of mean diameter a) and the contact angle at identified points on the circumference. At the forward edge, θ is taken as zero and is assumed to increase smoothly to the rear where $\theta = \theta_a$. Winterton [9] has studied a similar situation for a static gas bubble and recommends a sinusoidal relationship for θ at intermediate points. For our case the expression which fits the conditions is given by

Table 1. Data on bubbles A and B used for Fig. 6

Frame number	1	8	13	17	21	25	29	37
Time (ms)	0	1.94	3.33	4.44	5.56	6.67	7.78	10.00
Bubble A ($U_b = 0.58\ ms^{-1}$)								
Diameter D (mm)		1.5	1.7	1.9	2.1	2.2	2.3	~2.5
Height x (mm)		1.1	1.1	1.2	1.2	1.3	1.4	~1.6
Bubble B ($U_b = 0.55\ ms^{-1}$)								
Diameter D (mm)	1.9	2.2	2.4	2.7	out of view			
Height x (mm)	1.2	1.3	1.5	~1.7				

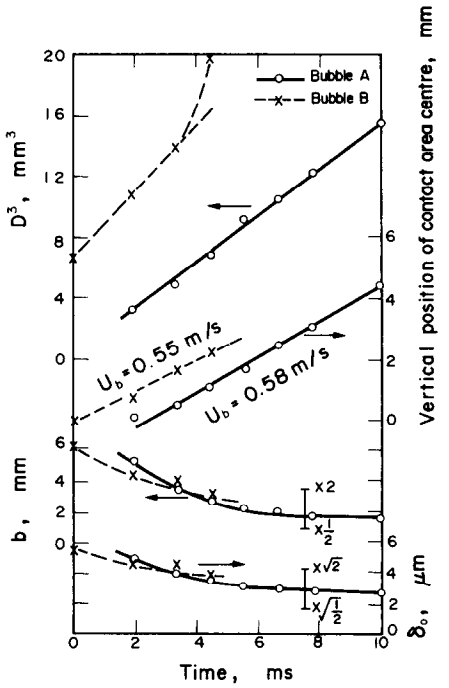

FIG. 6. Parameters for equations (6) and (7) bubbles A and B (Tolerances indicate effect of × 2 variation of b).

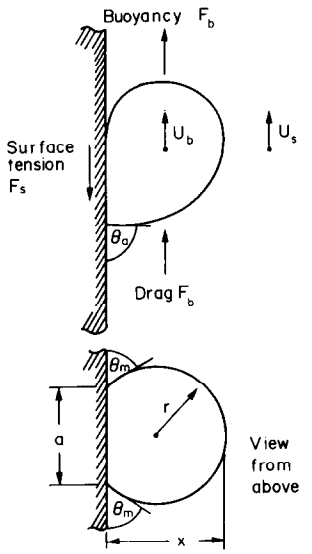

FIG. 7. Forces acting on a sliding bubble, $U_s > U_b$.

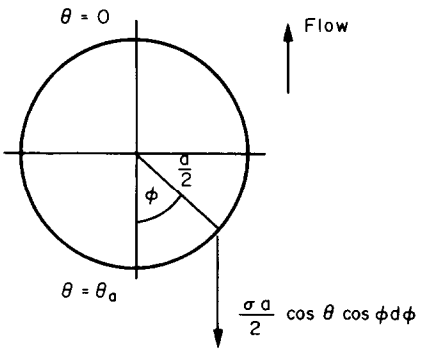

FIG. 8. Surface tension force on bubble base.

$$\cos\theta = \left(\frac{\cos\theta_a + 1}{2}\right) + \left(\frac{\cos\theta_a - 1}{2}\right)\cos\phi. \quad (9)$$

The surface tension force is given by

$$F_s = -\int_0^{2\pi} \tfrac{1}{2}\sigma\, a\cos\theta\cos\phi\, d\phi$$

which yields

$$F_s = (\pi/4)\sigma\, a(1 - \cos\theta_a).$$

At $\phi = \pi/2$, $\theta = \theta_m$ (Fig. 7) and equation (9) gives

$$\cos\theta_m = 1/2(\cos\theta_a + 1). \quad (10)$$

Also $$a = 2r\sin\theta_m.$$

Thus $$F_s = \pi\sigma r\sin\theta_m(1 - \cos\theta_m)$$

The other forces may be written as

$$F_b = (\pi r^3/3)(1 + \cos\theta_m)^2(2 - \cos\theta_m)\rho_f g \quad (11)$$

$$F_d = \frac{C_d\rho_f}{2} r^2(U_s - U_b)^2(\pi - \theta_m + \sin\theta_m\cos\theta_m) \quad (12)$$

where C_d is the drag coefficient of a sphere under the same conditions.

From

$$F_d = F_s - F_b$$

it follows that, for $U_s > U_b$,

$$(\Delta U)^2 = \frac{2\pi}{C_d}\left[\frac{N}{r}\left(\frac{\sigma}{\rho_f}\right) - \frac{Mgr}{3}\right] \quad (13)$$

where $\Delta U = U_s - U_b$ and M and N are both functions of θ_m only

$$M = \frac{(1 + \cos\theta_m)^2(2 - \cos\theta_m)}{\pi - \theta_m + \sin\theta_m\cos\theta_m}$$

$$N = \frac{\sin\theta_m(1 - \cos\theta_m)}{\pi - \theta_m + \sin\theta_m\cos\theta_m}.$$

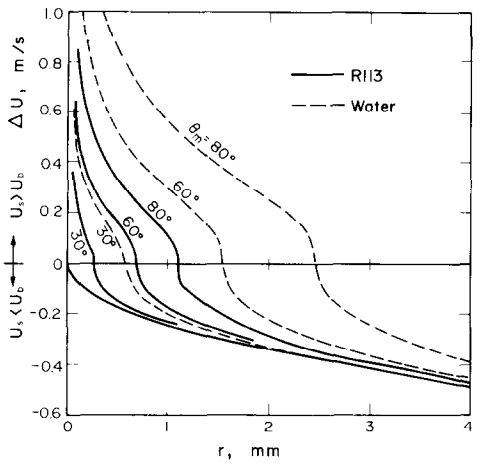

FIG. 9. Theoretical variation of ΔU with r for R113 and water at their atmospheric boiling points.

When $U_s < U_b$, F_d acts in the opposite direction to that shown and

$$(\Delta U)^2 = \frac{2\pi}{C_d}\left[\frac{Mgr}{3} - \frac{N}{r}\left(\frac{\sigma}{\rho_f}\right)\right]. \tag{14}$$

The balance is only strictly allowable under conditions when the bubble is moving ($U_b > 0$) as, under static conditions, the retarding contact angle (at the leading edge) is not approximately zero.

Reynolds number for bubbles in the millimetre range in normal liquids is between 10^3 and 10^5 and over this range $C_d = 0.45 \pm 0.08$. The only fluid dependent group is the ratio (σ/ρ_f) which is equal to $12.2 \times 10^{-6}\,\mathrm{Nm^2\,kg^{-1}}$ for R113 and $61.9 \times 10^{-6}\,\mathrm{Nm^2\,kg^{-1}}$ for water at their atmospheric boiling points. The variation of velocity difference (between the bubble and free stream) with r for each liquid, from equations (13) and (14) is shown in Fig. 9. The curves are drawn for various values of contact angle θ_m and it is assumed that contact is continuously maintained with the vertical wall. When the liquid is stagnant the $U_b > U_s$ curves give the rise velocity of the bubble at the wall and although the curves are not applicable when $U_b = 0$, the steepness as $U_b \to 0$ means that the intersection at $\Delta U = 0$ is effectively the bubble radius at the initial point of sliding. As the vertical liquid velocity is increased the radius at the initial point of sliding decreases.

Attempts to draw practical conclusions from the graph are somewhat hampered by the sensitivity to surface tension effects. Our photographic studies in R113 (and also those of Williams and Mesler [11] in water) indicate an angle θ_a behind the bubble of around 90°, implying $\theta_m \simeq 60°$. Both Gunther [3] and Akiyama and Tachibana [10] report sliding bubbles of around 1 mm radius in subcooled flowing water. The bubbles studied by Williams and Mesler [11] start to move upwards in the stationary water at a mean radius of 1.5–2.0 mm which may be compared to the prediction of 1.56 mm at $\theta_m = 60°$ from Fig. 9. Bubble A in this study has a mean velocity difference ΔU of 1.2 (± 30%) minus 0.58 (± 10%) $\mathrm{ms^{-1}}$ in other words somewhere in the range 0.20–1.04 $\mathrm{ms^{-1}}$. For this range Fig. 9 indicates a radius of less than half the experimentally observed radius (~ 1 mm). The difference is presumably due to the neglect of inertia effects (for bubble A, $\dot{R} \simeq 0.22\,U_b$ from Fig. 6) and geometrical complications caused by the curved surface. Finally it is interesting to note the prediction of generally larger bubbles in water than R113 and this may partially account for the large sliding bubbles observed by Niels [6]. (Very recently Al-Hayes and Winterton [13] have found $C_d = 1.22$ for attached air bubbles at $Re > 20$. This C_d value would affect the ΔU scale of Fig. 9 by a factor of 0.61.)

5. THE EFFECT OF SLIDING BUBBLES ON HEAT FLUX

The part of the total heat flux due to sliding bubbles may be estimated by using equation (8). The average number n_{sb} of sliding bubbles per unit sliding area on the surface at any one time may be expressed as the product of the number $\dot{n}_{sb}$ of sliding bubbles (from the main flow and nucleation) arising per unit time and area and the mean time τ_{sb} for which they slide on the surface,

$$n_{sb} = \dot{n}_{sb}\,\tau_{sb}.$$

If P is the mean proportion of the tube circumference over which the bubbles slide at mean velocity U_b on each side

$$\tau_{sb} = \frac{P\pi D}{2U_b}$$

and substitution into equation (8) gives

$$q_{sb} \simeq \dot{n}_{sb}\frac{P\pi D}{2}\rho_f h_{fg}\,a\,\delta_0. \tag{15}$$

An order of magnitude estimation (only) of the heat flux, based on the total area, which is due to sliding bubbles may now be made from the film. The film indicates that, for the width of tube in focus (~ 5 mm), sliding bubbles appeared with a frequency of about $100\,\mathrm{s^{-1}}$ each side of the tube. For bubble A, with $P = 0.5$ (in S.I. units),

$$q_{sb} \simeq \frac{100 \times 2}{0.005 \times 0.0191\,(\pi/2)} \times \frac{0.5\pi \times 0.0191}{2}$$

$$\times 1509 \times 145.7 \times 0.0015 \times 3.0 \times 10^{-6} \simeq 20\,\mathrm{kW\,m^{-2}}$$

This order of magnitude estimation shows that it is feasible for the sliding bubble mechanism to account

for most of the total measured heat flux (of $20\,kW\,m^{-2}$) at the upper tubes. In other words the increase in h (or decrease in ΔT_{sat}) by a factor of about four over that for the lower tubes at the same heat flux is mainly due to the large number of sliding bubbles around the upper tubes.

Now that sliding bubbles have been observed, a long term programme aimed specifically at the study of this phenomenon has been commenced. It is hoped that this will lead to more precise data on the sliding mechanism and the conditions under which it occurs.

6. CONCLUSIONS

(1). Examination by high speed photography of the flow between the upper tubes of a horizontal reboiler tube bundle reveals the presence of a large number of small bubbles in a turbulent bubbly flow.

(2). Bubbles were observed to slide up the sides of the tubes and to grow at a high rate. These sliding bubbles either originate from nucleation sites at the base of the tubes or by impact on the tubes from the main stream.

(3). Analysis based on the observed growth rates of the sliding bubbles correlates with the concept of a microlayer under the bubble. This microlayer has a thickness of a few micrometers and is less than that observed under some conditions of pool boiling.

(4). A force balance on the sliding bubble indicates that the bubble velocity is very sensitive to the property group (σ/ρ_f) and the contact angle.

(5). The feasibility of the sliding bubble mechanism accounting for the reported enhancement in heat transfer at the upper tubes has been shown.

(6). The results reported here apply to the small-bubbled foamy flow observed (and believed to occur in industrial reboilers). They are not applicable to large bubble or slug flow between the tubes nor to high voidage flow.

Acknowledgements—This work was sponsored by the Heat Transfer and Fluid Flow Service (HTFS) and was conducted as part of a research contract between the National Engineering Laboratory (NEL), Glasgow and the Heriot-Watt University, Edinburgh. The authors are grateful for helpful discussions with staff at Oxford University and NEL.

REFERENCES

1. L. S. Leong and K. Cornwell, Flow boiling heat transfer coefficients in a kettle reboiler tube bundle. *Chem. Engr. Lond.* **343,** 219 (1979).
2. K. Cornwell, N. W. Duffin and R. B. Schüller, An experimental study of the effects of fluid flow on boiling within a kettle reboiler tube bundle, Paper No. 80-HT-45, *ASME/AIChE National Heat Transfer Conf.* Orlando (1980).
3. F. C. Gunther, Photographic study of surface-boiling heat transfer to water with forced convection, *Trans. Am. Soc. Mech. Engrs.* **73,** 115 (1951).
4. G. H. Anderson and D. E. Minns, Nucleate boiling in a flowing liquid, 4th *Int. Heat Transfer Conf.* Paris, Paper No. B4.1 (1970).
5. K. I. Nakajima, Boiling heat transfer outside horizontal multitube bundles, *Heat Transfer Jap. Res.* **7,** 1–24 (1978).
6. G. H. Niels, Doctoral thesis, University of Delft, Netherlands, (1976); (See also Ch. 29th *Turbulent Forced Convection in Channels and Bundles* (edited by S. Kakaç and D. B. Spalding) Hemisphere (1979.
7. M. G. Cooper and A. J. P. Lloyd, The microlayer in nucleate pool boiling, *Int. J. Heat Mass Transfer* **12,** 895–913 (1969).
8. K. Cornwell, On boiling incipience due to contact angle hysteresis, *Int. J. Heat Mass Transfer* **25,** 205–211 (1982).
9. R. H. S. Winterton, Sizes of bubbles produced by dissolved gas coming out of solution on the walls of pipes in flowing systems, *Chem. Engng Sci.* **27,** 1223 (1972).
10. M. Akiyama and F. Tachibana, Motion of vapour bubbles in a subcooled heated channel, *Bull. J.S.M.E.* **17,** 241 (1974).
11. D. D. Williams and R. B. Mesler, The effect of surface orientation on delay time of bubbles from artificial sites during nucleate boiling, *A.I.Ch.E.Jl* **13,** 1020–1024 (1967).
12. K. Mori, Behaviour of vapour bubbles growing at a wall with forced flow, M.Sc. thesis, Oxford (1980).
13. R. A. M. Al-Hayes and R. H. S. Winterton, Bubble diameter on detachment in flowing liquids, *Int. J. Heat Mass Transfer* **24,** 223 (1981).

ETUDE PAR PHOTOGRAPHIE ULTRARAPIDE DE L'EBULLITION EXTERNE POUR UNE GRAPPE DE TUBES

Résumé—Un film à grande vitesse de l'ébullition à l'extérieur de tubes près du sommet d'un faisceau de tubes horizontaux révèle une multitude de petites bulles qui croissent rapidement tandis qu'elles montent en glissant contre les flancs du tube. Ces bulles proviennent à la fois de l'écoulement principal et de sites de nucléation à la base du tube. La vitesse de croissance mesurée s'accorde bien avec la théorie basée sur une microcouche en évaporation sous la bulle. On montre que les bulles glissantes sont responsables de l'accroissement du transfert de chaleur qui est observé sur les tubes supérieurs de la grappe.

UNTERSUCHUNG DER VERDAMPFUNG AN EINEM ROHRBÜNDEL MITTELS HOCHGESCHWINDIGKEITS-FOTOGRAFIE

Zusammenfassung—Ein Hochgeschwindigkeitsfilm vom Sieden an den obersten Rohren eines horizontalen Verdampfer-Rohrbündels zeigt eine Vielzahl kleiner Blasen, die während des Emporgleitens an den Rohrflanken schnell wachsen. Diese Blasen stammen sowohl aus dem Hauptstrom wie auch von Keimstellen an der Unterseite des Rohres. Die gemessene Wachstumsgeschwindigkeit stimmt gut mit der nach der Theorie einer verdampfenden Mikroschicht unter der Blase überein. Es wird gezeigt, daß diese gleitenden Blasen die beobachtete Vergrößerung des Wärmeübergangs an den oberen Rohren des Bündels erklären können.

ИССЛЕДОВАНИЕ КИПЕНИЯ НА ВНЕШНЕЙ СТОРОНЕ ПУЧКА ТРУБ МЕТОДОМ ВЫСОКОСКОРОСТНОЙ КИНОСЪЕМКИ

Аннотация — Высокоскоростная киносъемка процесса кипения на внешней стороне верхней части горизонтального пучка труб кипятильника обнаруживает множество небольших пузырьков, которые быстро растут и скользят вверх по стенкам трубы. Пузырьки зарождаются как в основном потоке, так и в центрах образования пузырьков на нижней стенке трубы. Измеренные значения скорости роста пузырьков хорошо согласуются с рассчитанными по методу испаряющегося микрослоя под пузырьками. Показано, что скольжением пузырьков можно объяснить интенсификацию теплопереноса в верхней части пучка.